

SUPPLEMENTAL MATERIAL INFORMATION

Legends to Supplemental Figures

Supplemental Figure 1. Expression of p110 isoforms in pancreatic cancer cell lines. (A, B) Analysis of p110 isoforms and its regulatory subunit expression by western-blot in 5 human pancreatic cancer cell lines and 7 primary murine *Kras*^{G12D}-driven PanINs or PDAC cell lines with and without *p53*^{R172H} expression as described in D. (C) Regentyping of mouse cell lines from GEMMs by PCR (Hingorani et al. 2005). (D) Origin of the murine cell lines.

Supplemental Figure 2. Validation of Cre-induced recombination of *Pik3ca* gene in pancreata only. (A) Schematic representation of conditional *Pik3ca* gene targeting: the genetically modified allele is represented before ($p110\alpha^{lox}$) and after Cre recombination ($p110\alpha^{\Delta DFG}$) (Graupera et al. 2008). DFG is a conserved motif in the activation loop of the p110 α kinase domain critical for the activity. The gene targeting strategy used is different from a traditional conditional knock-out strategy. Instead, it is deleting two exons in the catalytic domain of *Pik3ca* in the 3' part of the gene, allowing expression of a truncated inactive p110 α after recombination (Graupera et al. 2008). Red lines correspond to the pair of genotyping primers (pre-cre primers): FE1 - GGATGCGGTCTTTATTGTC; FE4 - TGGCATGCTGCCGAATTG; annealing temperature: 65°C; wild type (+)-640bp, lox-708bp. Blue lines corresponds to post-cre primers used to verify the presence of recombined allele ΔDGF : ma9 - ACACACTGCATCAATGGC; a5 = GCTGCCGAATTGCTAGGTAAGC; annealing temperature: 65°C; recombined ΔDGF -544 bp, wild type (+) or unrecombined lox- >10kpb amplicon. (B) Genotyping of tail samples. Detection of LSL-Kras allele; detection of Pdx1-Cre transgene, as described (Hingorani et al. 2003); detection of *pik3ca* alleles (FE1/FE4 primers). (C) Validation of specific cre recombination of *pik3ca* gene in the pancreas by PCR on genomic DNA. Samples from liver were used as a negative control. As expected, the recombined allele $p110\alpha^{\Delta DFG}$ is observed in cre expressing tissue only

(pancreas): full recombination in KC;p110 α ^{lox/lox} and partial recombination in KC;p110 α ^{+/lox} is demonstrated by respectively the absence of the lox allele or presence of the WT allele. (D) WB using indicated antibodies on 2 month-old pancreatic lysates from indicated genotypes (left panel). Relative quantification is shown in the right panel (N=9 for each genotype). Isoform-specificity of antibody was previously shown in (Guillemet-Guibert et al. 2008). Full recombination of lox allele was verified for all samples as shown for the samples presented here (lower panel).

Supplemental Figure 3. p110 α inactivation with and without Kras activation does not lead to Langerhans islet defects or to mouse lethality, but blocks Kras induced pancreatic carcinogenesis. (A) Hematoxylin and eosin staining of pancreas sections from 6 month-old p110 α ^{lox/lox} and C;p110 α ^{lox/lox} mice. Scale=200 μ m. (B) IHC analysis of insulin, glucagon and somatostatin in 6 months-old p110 α ^{lox/lox} and C;p110 α ^{lox/lox} mice. Quantification of the percentage of glucagon and somatostatin positive cells is shown in the lower panel (quantification was performed on 5 Langerhans islets per mice, N=4 mice for each genotype, Student's t-test). Considering the crucial role of p110 α in glucose metabolism and insulin receptor adaptors IRS1/2-mediated signalling (Foukas et al. 2006; Vanhaesebroeck et al. 2010), we confirmed that the cell repartition of the endocrine compartment was unchanged after inactivation of p110 α in the pancreas. In particular, in contrast with IRS2 knock-out, glucagon-positive cells were present (Kubota et al. 2000). Scale=100 μ m. (C) Homozygous inactivation of p110 α in the pancreas did not significantly affect circulating levels of glucose or insulin of young randomly fed mice (N>11; 7-week old; ns, Mann-Whitney test) nor body weight (not shown). (D) Quantification of ADMs and PanINs in KC;p110 α ^{+/lox} (N=12) and KC;p110 α ^{lox/lox} mice (N=14; 6 month old; *p<0.05, Mann-Whitney test). The percentage of ADM or PanIN1 surface over total pancreatic surface was quantified for each mouse. Each point represents a single mouse, and horizontal bars represent mean percentage for each group. P values are < 0.05 Mann-Whitney test. (E) Hematoxylin and eosin and IHC staining of recombined KC;p110 α ^{lox/lox} pancreas sections from 6 month-old KC;p110 α ^{lox/lox} mice harboring low grade PanINs lesions. These lesions are devoid of

surrounding fibrous reaction (arrow heads). Scale=200 μ m (H&E); 100 μ m (IHC stainings). (F) Recombination of *pik3ca* locus was verified in these PanIN lesions after microdissection of paraffin embedded 4 μ m sections (hematoxylin counterstain) by analyzing the disappearance of the lox allele by nested PCR after DNA extraction; T corresponds to tail DNA from KC;p110 $\alpha^{lox/lox}$. Genotyping CRE PCR was used as a control for DNA extraction. First sample was dissected twice with similar results.

Supplemental Figure 4. p110 α activity is crucial for induction and maintenance of pancreatic ADM/PanIN lesions induced by inflammation in the context of mutated *Kras*. Representative IF or IHC of pancreata of indicated genotype, 1 day (A, B, C) or 5 days (B, C) after the last caerulein or vehicle injection using indicated antibodies (N=3 for each group). For quantification, each point represents the mean of 5 fields per mouse (N=3, magnification x20, ** p<0.01 Student's t-test). Black arrowheads show positively stained-cells. (A) Scale=10 μ m. (B) Ki67=Scale=100 μ m (C) Scale= 90 μ m. (D) Scale=500-90 μ m. (E) Schematic representation of the role of p110 α in inflammation-induced pancreatic injury and regeneration in the presence or absence of oncogenic *Kras*.

Supplemental Figure 5. Genetic inactivation of p110 α blocks ADM induction *ex vivo*. Phase contrast images of KC, KC;p110 $\alpha^{+/lox}$ and KC;p110 $\alpha^{lox/lox}$ acinar cells 6 days after isolation and treatment with TGF- α (50 ng/ml). Quantification of the percentage of ductal structures after 6 days in culture (*ex vivo* acinar cultures from independent mice; N=2 mice in triplicate; * p<0.05 , **p<0.01, Student's t-test). Scale=50 μ m.

Supplemental Figure 6. p110 α regulates actin cytoskeleton during inflammation-induced ADM and PanIN formation. (A) Lower magnification (x63) of confocal microscopic images of actin staining on paraffin-embedded pancreata in indicated conditions (N=3 per genotype). Positive controls for actin staining unchanged by pancreatic-specific p110 α inactivation are Langerhans islets (not shown). Scale=10 μ m. (B) F-actin network in A66 or vehicle treated transdifferentiated acinar cells *in vitro*.

Representative signal intensity scans across cell is shown. Scale=10 μ m. (C) WB in KC;p110 $\alpha^{+/lox}$ versus KC;p110 $\alpha^{lox/lox}$ mice and sacrificed 1 day after last caerulein or PBS injection. Quantification of all samples (N>2).

Supplemental Figure 7. p110 α is a critical signalling hub in pancreatic preneoplastic lesion initiation. (A) Ras *in vivo* activity from pancreatic lysates of KC;p110 $\alpha^{+/lox}$ compared to KC;p110 $\alpha^{lox/lox}$ mice (N=3), sacrificed 1 day after last caerulein injection. Relative quantification of all mice analyzed is shown below (* p<0.05, Student's t-test). Positive and negative controls correspond respectively to GTP and GDP loading of Raf1-RBD (not shown). (B) IHC with anti-NF- κ B/p65 antibodies in indicated conditions (8h after caerulein treatment). Scale=10 μ m. For quantification, each point represents the mean of 5 fields per mouse (N \geq 3, **p<0.01, Student's t-test). (C) Quantification of pSTAT3-positive nuclei in indicated conditions. For quantification, each point represents the mean of 5 fields per mouse (N=3, **p<0.01, Student's t-test, versus KC). (D) Relative quantification of pSTAT3 and EGFR in all mice analyzed by western-blot is shown (N \geq 3; * p<0.05, Student's t-test).

Supplemental Figure 8. Full p110 α inactivation in the KPC model results in preneoplastic lesions with decreased activation of key signalling pathways. (A) Genotyping for recombined *Pik3ca* allele in PanIN lesions of KPC;p110 $\alpha^{lox/lox}$ mice. (B) Phenotypic characterization and analysis of signalling pathways activated in these lesions.

Supplemental Figure 9. p110 α specific inhibitor A66 decreases Akt/mTOR downstream signalling pathway in murine embryonic fibroblasts. After 24 h serum starvation, MEF cells with indicated stable transfections were pre-treated with p110 α specific inhibitor A66 (10 μ M) or vehicle during 1h and stimulated with 2%FBS during 10 min. Western-blot analysis was performed using indicated antibodies.

DETAILED EXPERIMENTAL PROCEDURES

Plasmatic dosage of insulin. Plasmatic levels of insulin in 7 week-old mice was measured using ELISA assay (Mercodia).

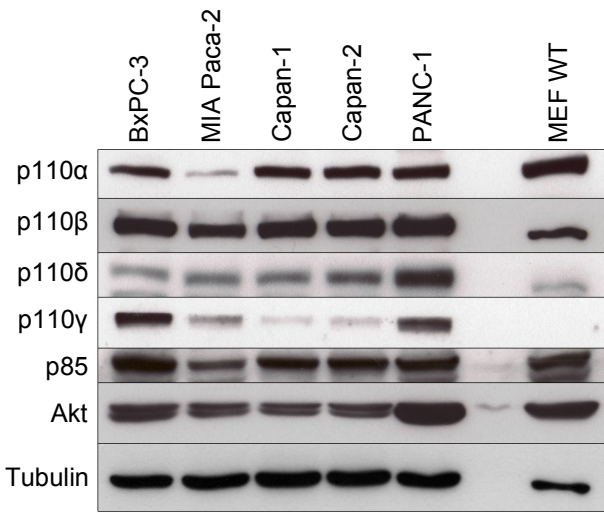
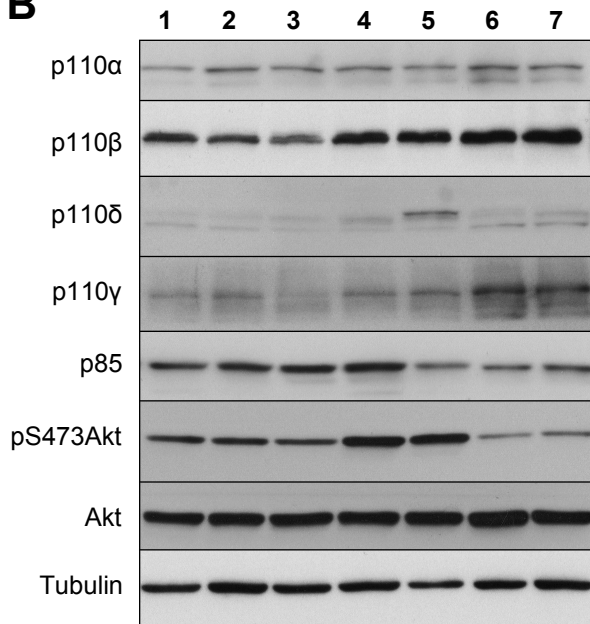
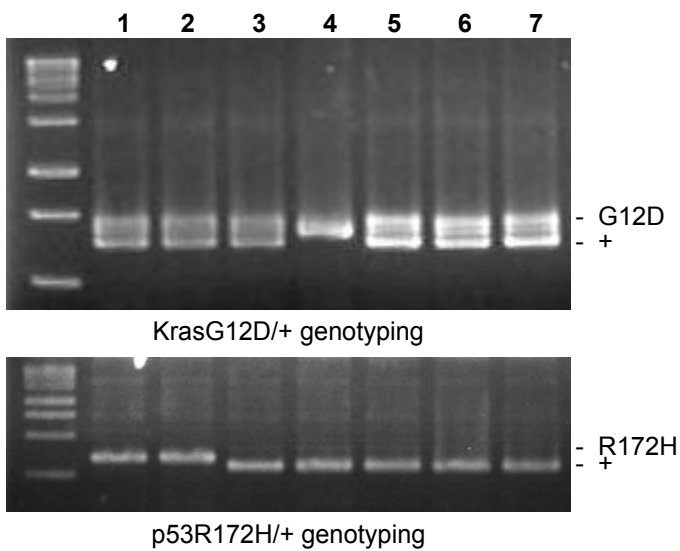
DNA extraction and PCR conditions for microdissected samples. DNA was extracted from hematoxylin stained 4µm FFPE sections; DNA extraction from Arcturus caps and PCR was performed using Sigma Redextract NAmpl. After first amplification using FE1/FE4 primers, a nested PCR was used using the following primers: nested FE1=TTGTCTCTTCTGTCCGATGT; nested FE4=TTGCTAGGTAAGCCTTGTAAC. 2 rounds of CRE PCR is used as a control for DNA extraction.

Antibodies and conditions

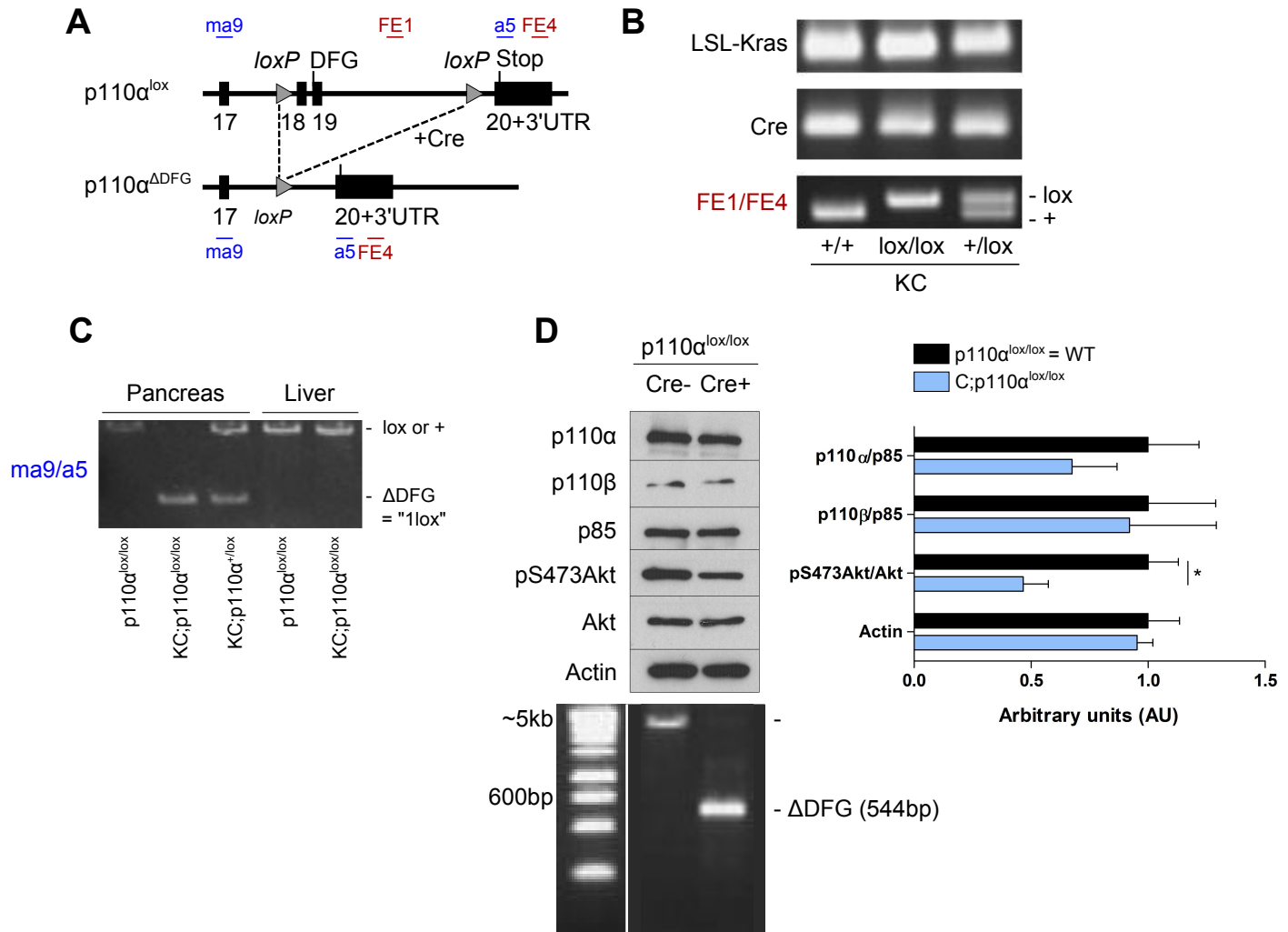
| Protein targeted | Origin | Targeted species | Company | Dilution | Fixation/ Antigen retrieval | Use |
|-----------------------|---------------|---------------------------------------|---------------------------------------|------------------|--------------------------------|----------|
| Amylase | Rabbit | Human, mouse, rat | Sigma A8273 | 1/1000 | PFA 3,7 % | IF |
| CAII | Rabbit | Human, rat | Gift, Fanjul M | 1/100 | PFA 3,7 % | IF |
| CK19 | Hybridome TR3 | rat | Gift, Gigoux V | 1/2 | PFA 3,7 % | IF |
| Trypsin | Sheep | NA | Gift, Fanjul M | 1/100 | PFA 3,7 % | IF |
| Phalloïdin-TRITC | NA | NA | SigmaP1951 | 1/500 | PFA 3,7 % | IF |
| Ab II anti-Rabbit | Goat | Rabbit | Lifetechnologies | 1/1000 | PFA 3,7 % | IF |
| Ab II anti-Rat FITC | Mouse | Rat | Interchim UPB91360 | 1/1000 | PFA 3,7 % | IF |
| Ab II anti-sheep HRP | Rabbit | Sheep | DAKO P0163 | 1/1000 | PFA 3,7 % | IF |
| pSer473 Akt | Rabbit | Human, mouse, rat | Cell Signaling Technologies, XP #4060 | 1/20 | Formalin, Citrate | IHC |
| pAkt Substrate | Rabbit | All | Cell Signaling Technologies, #9611 | 1/1000 | Formalin, Citrate | WB |
| pThr202/Tyr204 ERK1/2 | Rabbit | Human, mouse, rat | Cell Signaling Technologies, #4370 | 1/100 | Formalin, Citrate | IHC |
| Ki67 | Rabbit | Human | Epitomics, #4203-1 | 1/400 | Formalin, Citrate | IHC |
| CK19 | Rabbit | Mouse | Epitomics, #3863-S | 1/1000 | Formalin, Citrate | IHC |
| β-actin | Mouse | All | Sigma (AC-74) | 1/100 | Formalin, Citrate | IF |
| Amylase | Rabbit | | Sigma | 1/1000 1/3000 | Formalin, Citrate | WB IF |
| IL6 | Rabbit | | Abcam #6672 | 1/250 | Formalin, Citrate | IHC |
| αSMA | Mouse | Mouse, rat, rabbit, human, pig, sheep | Abcam, ab7817 | 1/250 | Formalin, Citrate | IHC |
| p65 | Rabbit | Human, mouse, rat, monkey,dog | Cell Signaling Technologies, #8542 | 1/200 | Formalin, Citrate | IHC |
| insulin | Guinea pig | Mouse, rat, bovine | BioGenex, AR029-5R/PU029-UP | none | Formalin, Citrate | IHC |
| glucagon | Mouse | Human, mouse, rabbit, rat | Sigma, G 2654 | 1/5000 | Formalin, Citrate | IHC |
| somatostatin | Rabbit | | Dako, A0566 | 1/300 | Formalin, | IHC |

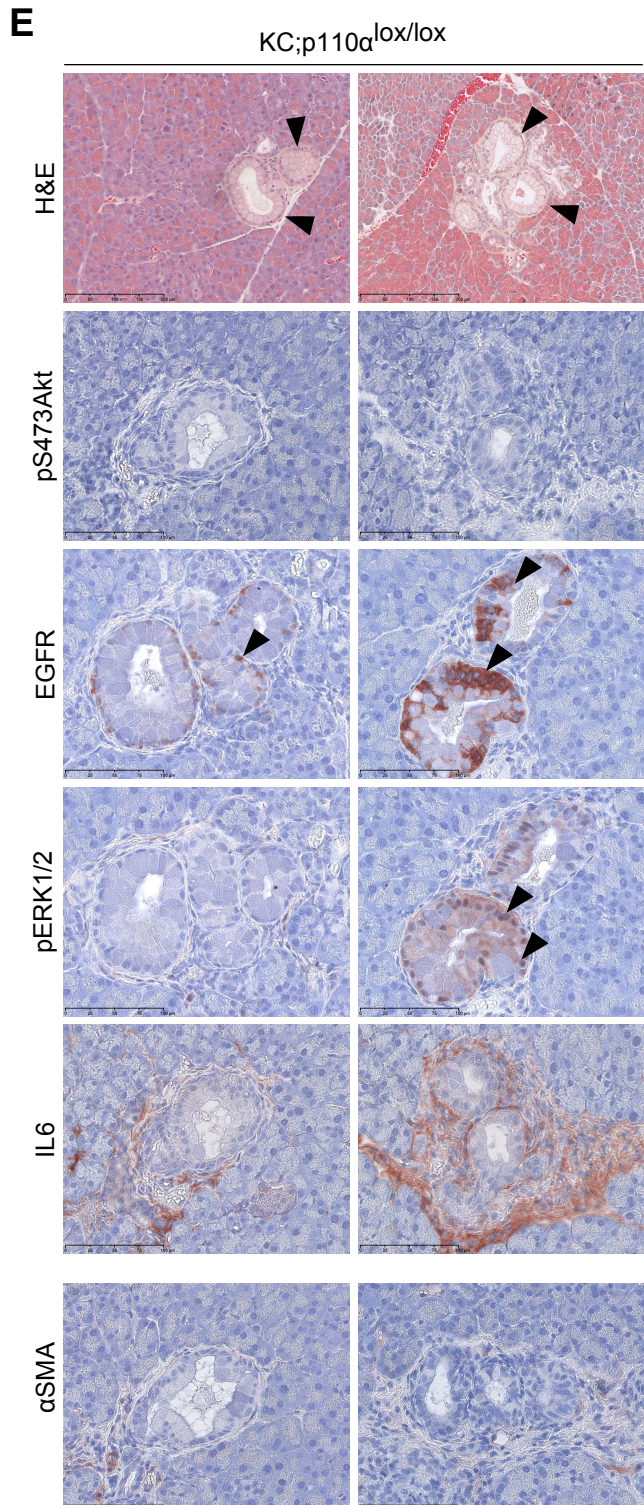
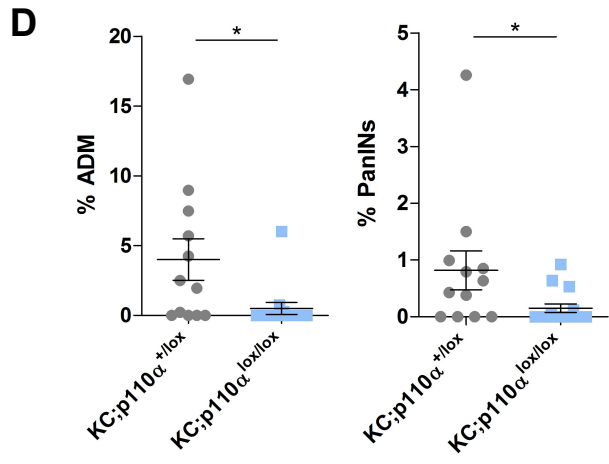
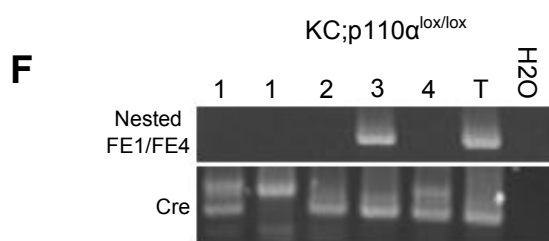
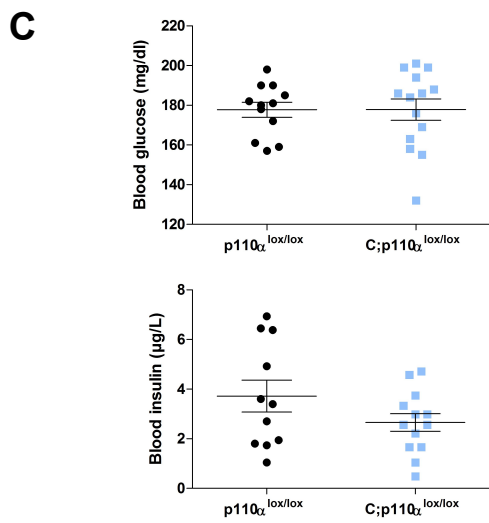
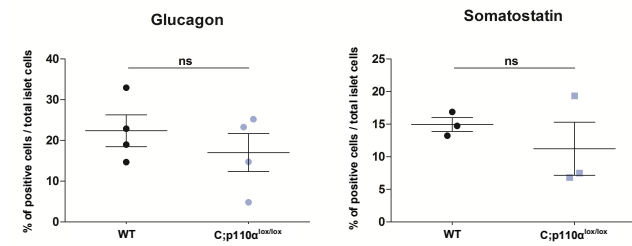
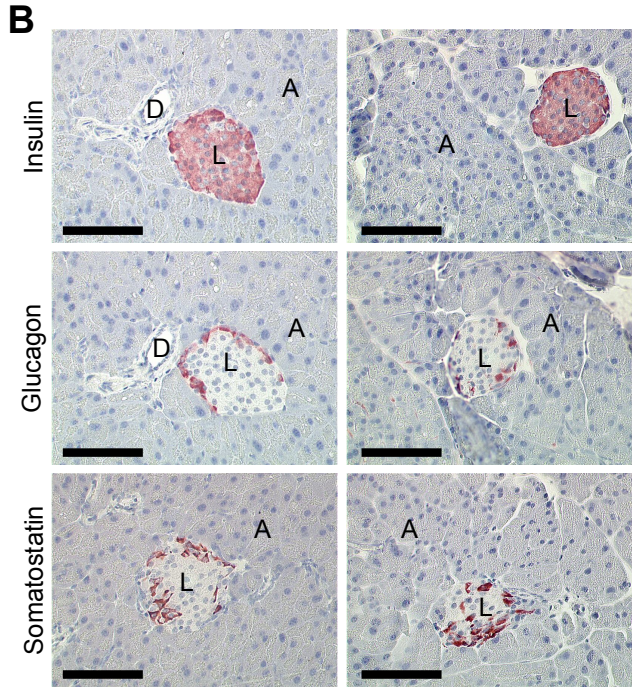
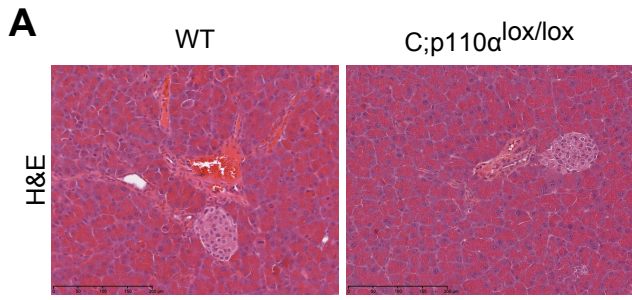
Baer, et al. -Supplemental data - 6 -

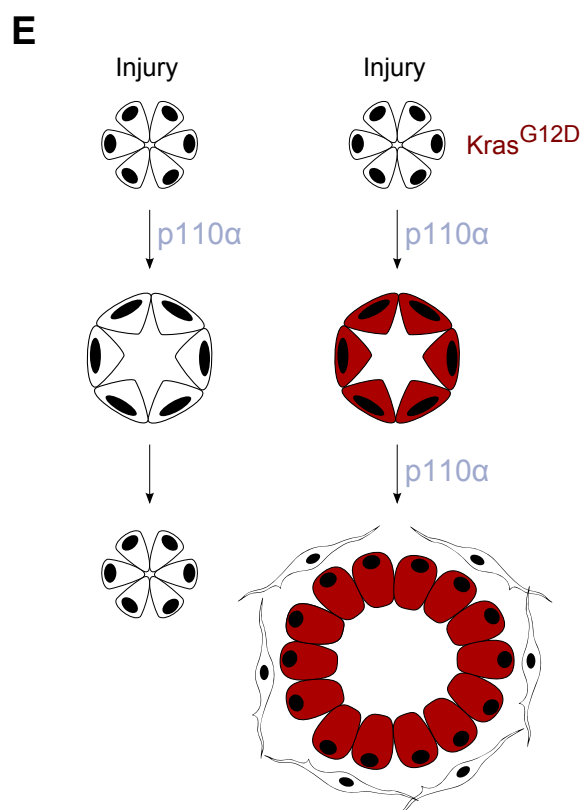
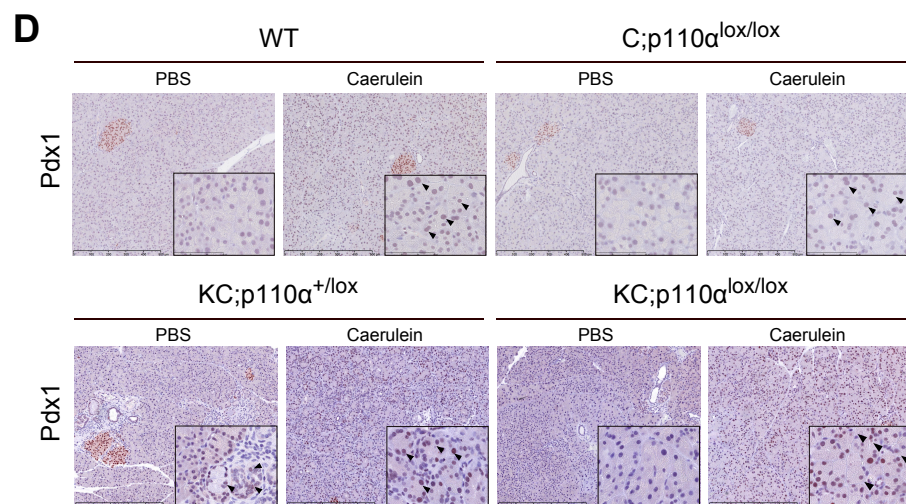
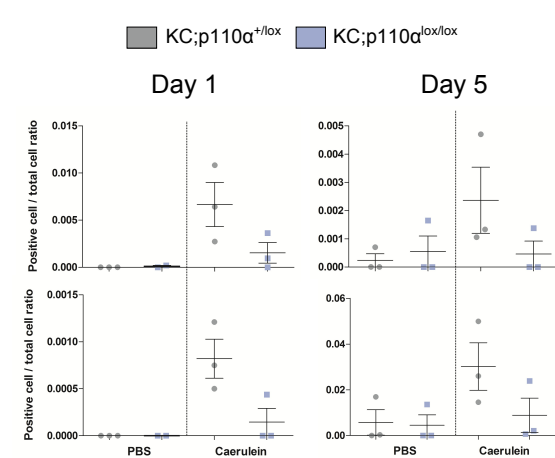
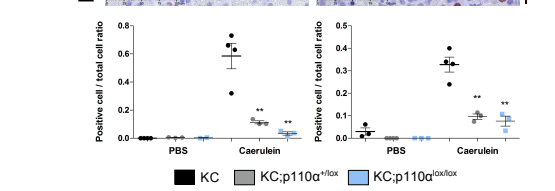
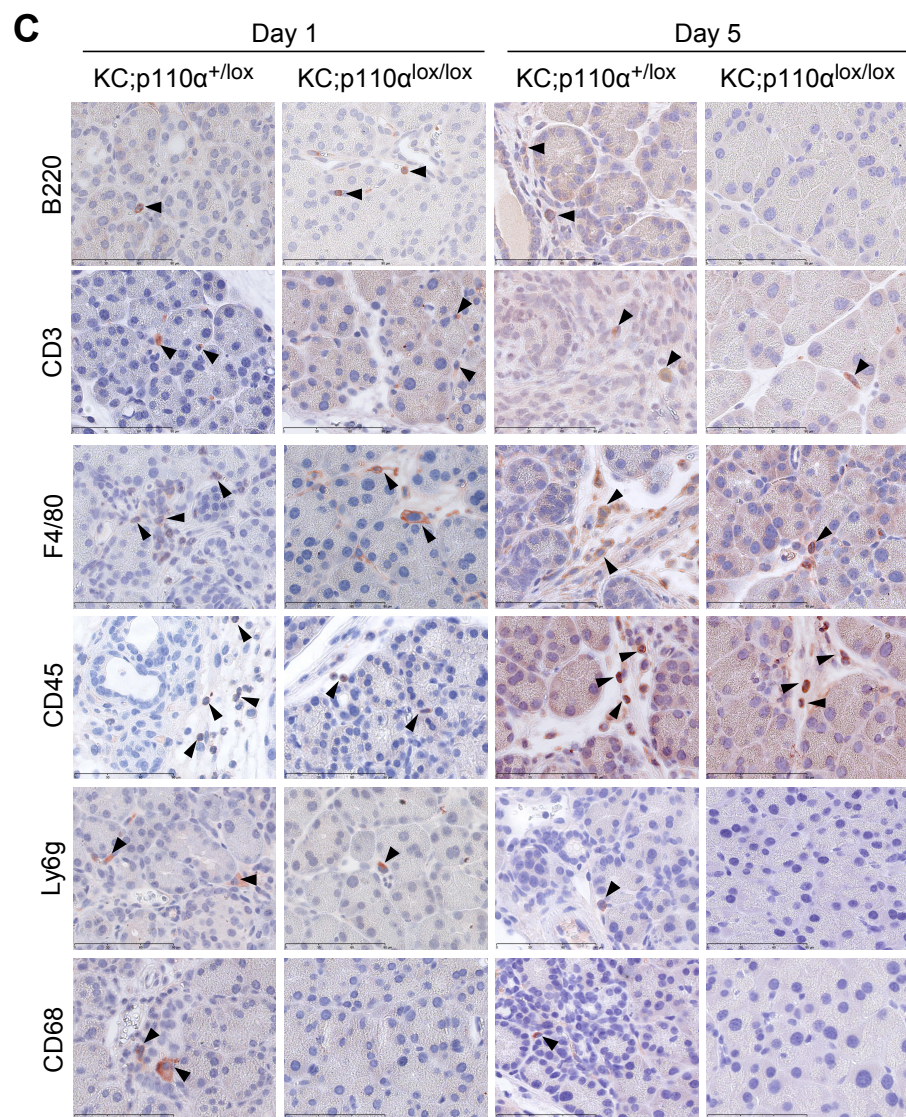
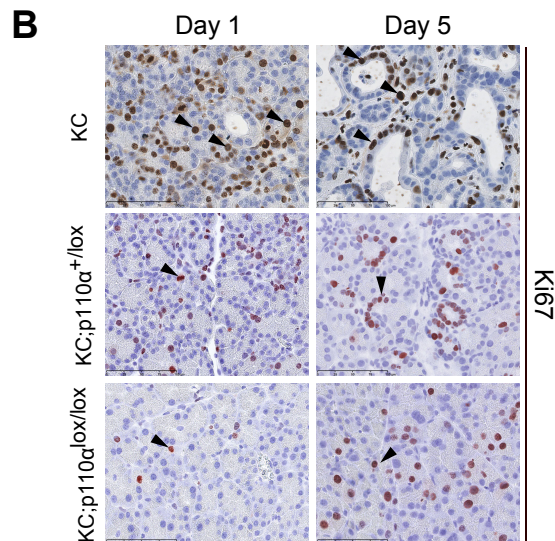
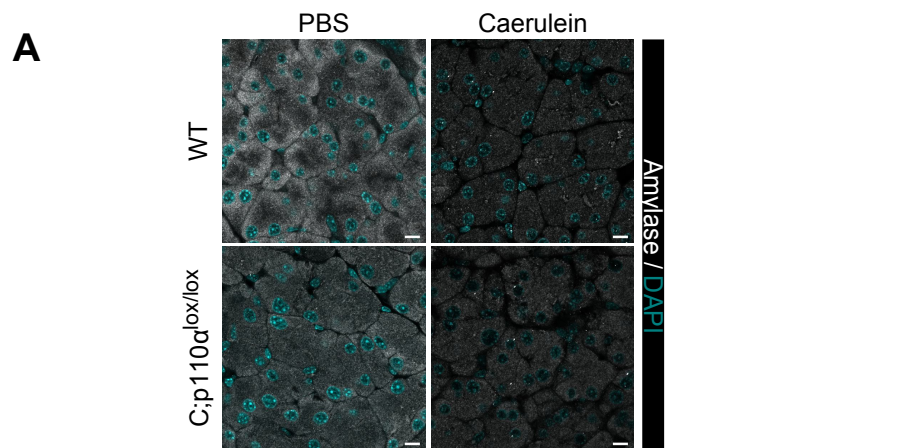
| | | | | | | |
|--------------------------------|--------|------------------------------|---------------------------------------|-------------|---------------------------|------------|
| pTyr705 STAT3 | Rabbit | Human, mouse, rat | Cell Signaling Technologies, #9145 | 1/100 | Citrate Formalin, EDTA | IHC, WB |
| EGFR | Rabbit | Human, mouse, rat | Epitomics, #1902-1 | 1/100 | Formalin, Citrate | IHC |
| CD45 | Rat | Mouse | R&D Systems, MAB114 | 1/5000 | Formalin, Citrate | IHC |
| B220 | Rat | Mouse | R&D Systems, MAB1217 | 1/1000 | Formalin, Citrate | IHC |
| LY6G | Rat | Mouse | Abcam, ab25377 | 1/3000 | Formalin, Citrate | IHC |
| CD3 | Rat | Mouse | R&D Systems, MAB4841 | 1/5000 | Formalin, Citrate | IHC |
| CD68 | Rat | Mouse | ABD serotech, MCA 1957 | 1/100 | Formalin, Citrate | IHC |
| F4/80 | Rat | Mouse | Abcam, ab6640 | 1/5000 | Formalin, Citrate | IHC |
| Pdx1 | Rabbit | Mouse, Rat, Cow, Dog, Human | Abcam | Ab47267 | Formalin, Citrate | |
| Ab II anti-rabbit | Rabbit | Rabbit | Cell Signaling Technologies, #8114 | - | Formalin | IHC |
| p85 | Rabbit | Rabbit, human, mouse, monkey | Millipore/ Upstate, 06-497 | 1/2000 | | WB |
| pThr246 PRAS40 | Rabbit | Human, mouse, rat, monkey | Cell Signaling Technologies, #2997 | 1/1000 | | WB |
| pSer240/244 S6 | Rabbit | Human, mouse, rat, monkey | Cell Signaling Technologies, XP #5364 | 1/1000 | | WB |
| p110α | Mouse | Human, rat | BD Bioscience 611398 | 1/500 | | WB |
| p110β | Rabbit | Human, mouse, rat | Santa Cruz, SC-602 | 1/1000 | | WB |
| p110γ | Rabbit | | In house kind gift from E. Hirsch | 1/2 in HBSS | | WB |
| p110δ | Rabbit | Human, mouse, rat | Santa Cruz, SC-7176 | 1/1000 | | WB |

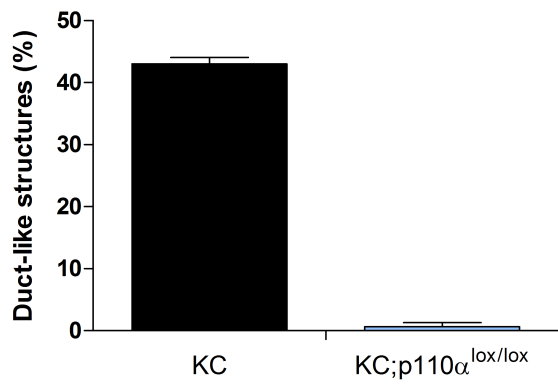
A**B****C****D**

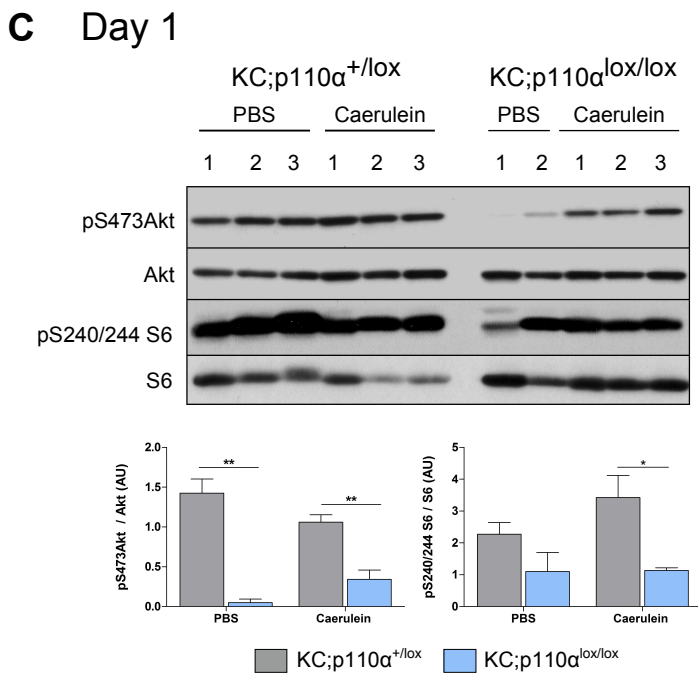
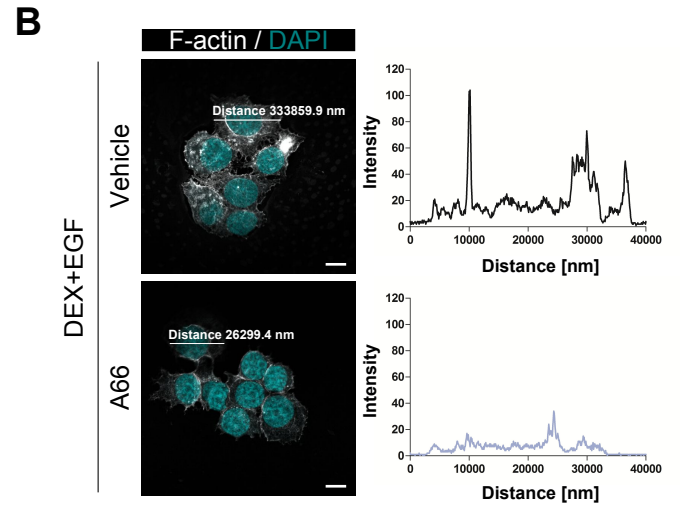
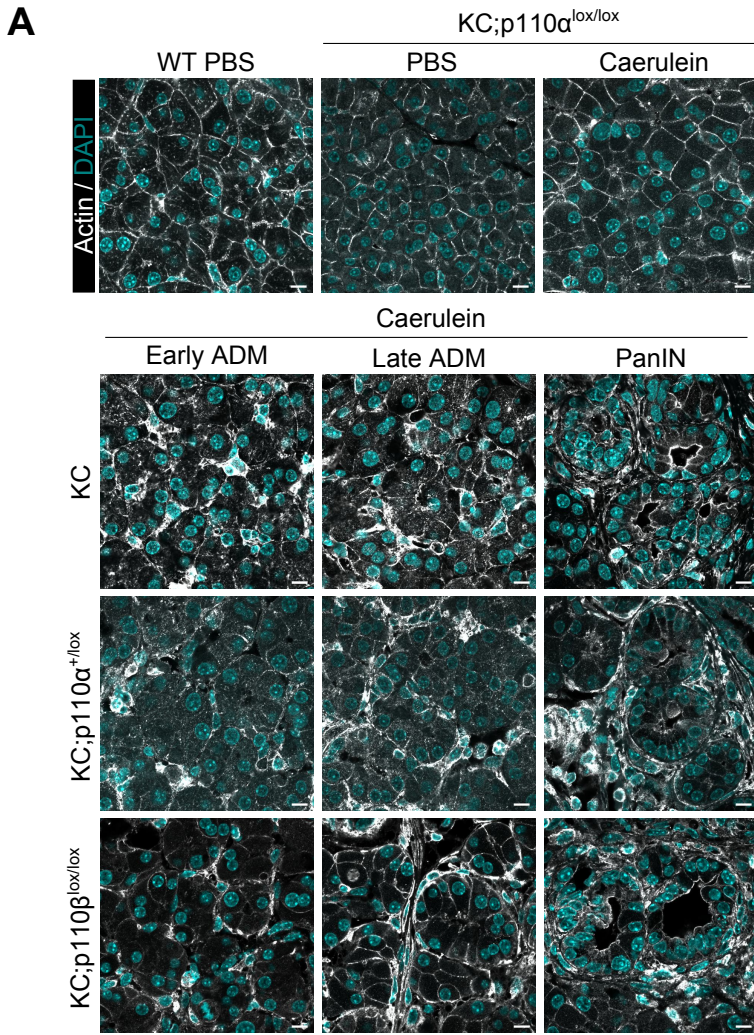
| Murine cell lines | 1 | 2 | 3 | 4 | 5 | 6 | 7 |
|-------------------|---|---|---|---|---|---|---|
| KrasG12D/+ | + | + | + | + | + | + | + |
| p53R172H/+ | + | + | | | | | |
| PDAC | + | + | | | + | + | + |
| PanIN | | | + | + | | | |

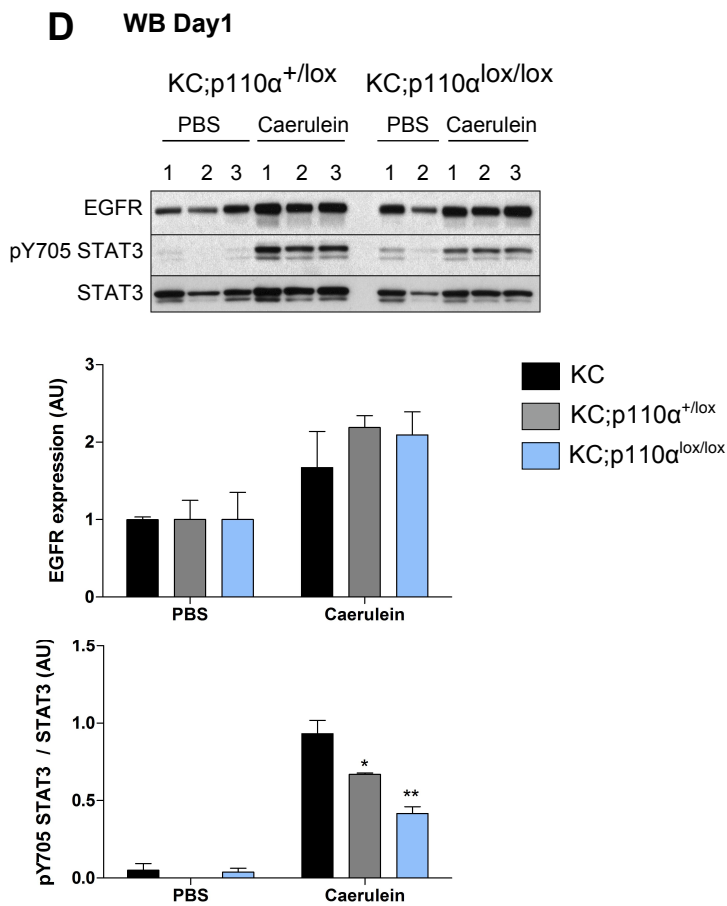
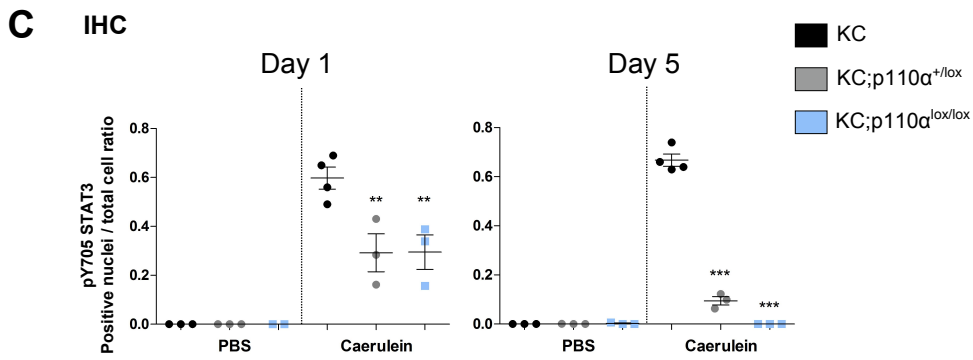
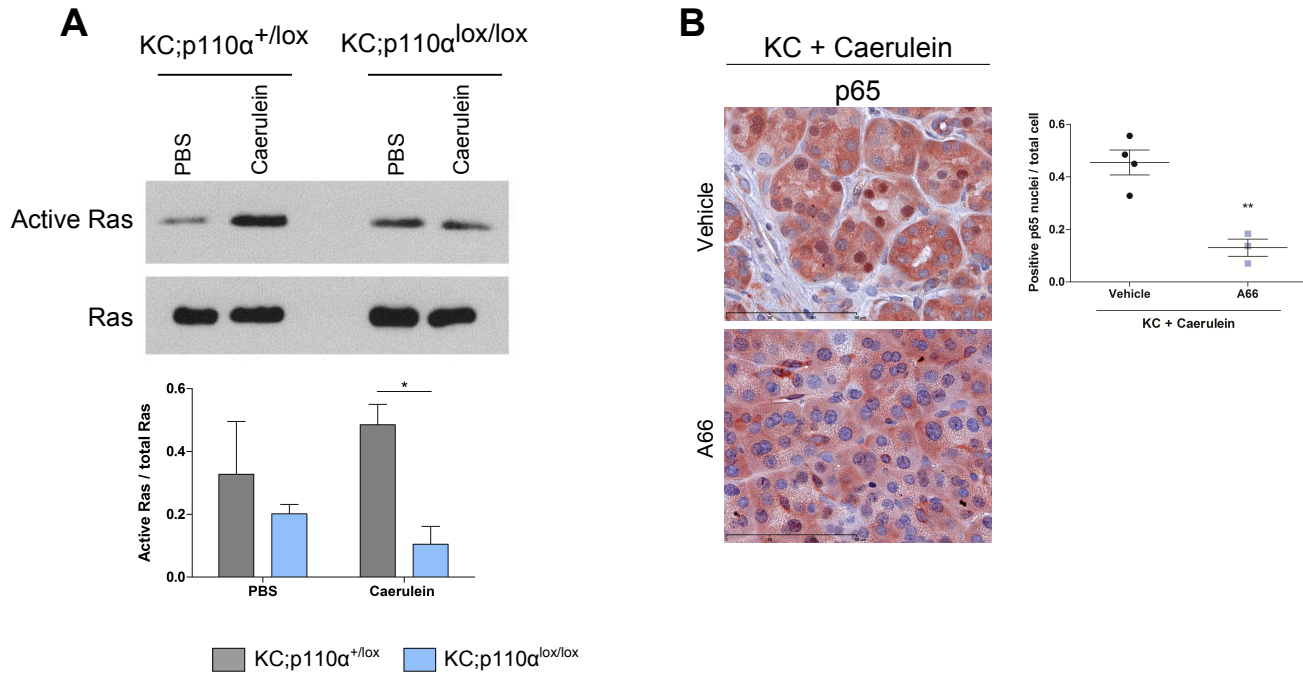


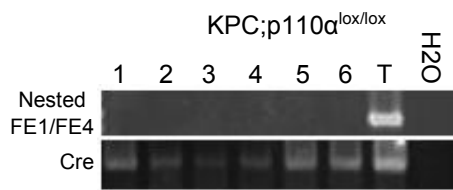
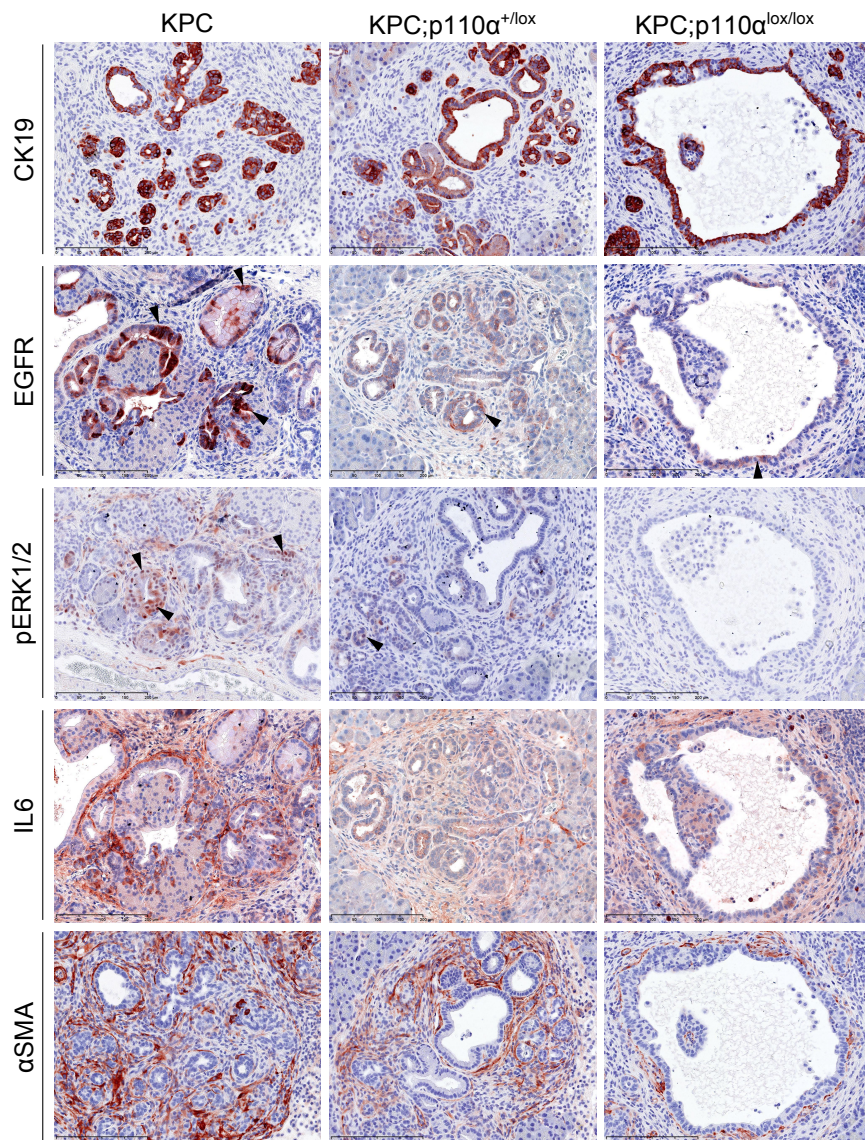




A





A**B**

A